

SINGLET OXYGEN GENERATION BY AN INDOTRICARBOCYANINE DYE WITH BULKY SUBSTITUENTS

M. P. Samtsov,^{a,*} D. S. Tarasov,^{a,b}
and E. S. Voropay^b

UDC 535.37;547.97;577.3;543.426

A study was carried out on the spectral-luminescence and phosphorescence properties of an indotricarbocyanine dye with an ortho-phenylene bridge in the conjugation chain as well as two 300-Da polyethylene glycol (PEG) substituents (PD1) and its analog without PEG (PD2). The presence of the bulky PEG300 substituents in the dye structures was shown to alter the efficiency of singlet oxygen generation. The yield of singlet oxygen in ethanol for both dyes in the concentration range from $5 \cdot 10^{-8}$ to 10^{-5} M has a constant value $\gamma_{\Delta} = 0.031 \pm 0.005$ for PD1 and 0.050 ± 0.008 for PD2. An increasing value of γ_{Δ} from 0.022 ± 0.004 when $C_{\text{dye}} = 2.6 \cdot 10^{-7}$ M to 0.104 ± 0.016 when $C_{\text{dye}} = 5.8 \cdot 10^{-5}$ M was found in the concentration range from 10^{-7} to 10^{-5} M in low-polarity chloroform for PD2, whereas the quantum yield for PD1 with bulky substituents is invariant in this concentration range (0.032 ± 0.003). The increase in the singlet oxygen formation quantum yield with increasing concentration of PD2 in low-polarity chloroform is attributed to an increase in the fraction of contact ion pairs in solution and a heavy atom effect related to the Br^- anion. The presence of two PEG300 chains in the structure of the cationic indotricarbocyanine dye (~770 Da) prevents the counterion from moving away from the cation of dye PD1 in low-polarity chloroform. Furthermore, the dye molecules are in the form of contact ion pairs at any concentration and it is hence difficult for the chromophore to interact with dissolved oxygen due to steric hindrance.

Keywords: indotricarbocyanine dyes, polyethylene glycol, ion pairs, photophysical properties, singlet oxygen, concentration effects.

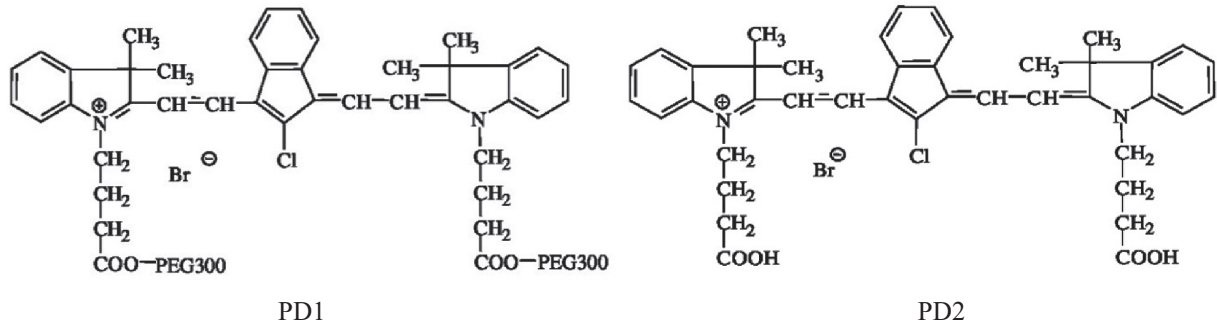
Introduction: In air-saturated solvents, some part of the excitation energy of polymethine dyes (PD) is consumed in the sensitization of singlet oxygen (${}^1\text{O}_2$) formation. The generation of ${}^1\text{O}_2$ accounts for the photodecomposition of these dyes [1, 2]. The efficiency of these dyes as photosensitizers (PS) for phototherapy depends to some extent on their capacity to generate ${}^1\text{O}_2$ [3–7]. In this regard, it is important to study the formation of ${}^1\text{O}_2$ molecules under conditions corresponding to biological tissues in order to elucidate the mechanism for photoactivity of new compounds. Since indotricarbocyanine dyes are located in cancer cells in regions of low dielectric constant [8, 9], low-polarity solvents are a suitable model medium. In such solvents, the properties of the microenvironment of the PD molecules most closely correspond to biological tissues, which permits us to compare the dissipation of electronic excitation energy in such systems.

In previous work [10–14], we showed that an indotricarbocyanine dye with an ortho-phenylene bridge in the conjugation chain and two terminal polyethylene glycol (PEG) substituents when used as a photosensitizer displays high efficiency in attacking cancer cells, accumulation selectivity, and low toxicity. In the present work, results are given for a study of the photophysical properties of this compound in organic solvents differing in polarity.

Experimental. We studied an indotricarbocyanine dye PD1 with a chlorine-substituted ortho-phenylene bridge in the polymethine conjugation chain covalently bonded to two PEG300 chains and its analog, dye PD2 without the PEG substituents. The counterion for both PD1 and PD2 is the Br^- anion.

^aA. N. Sevchenko Institute of Applied Physical Problems of Belarusian State University, Minsk, Belarus;

^bBelarusian State University, Minsk, Belarus. Translated from Zhurnal Prikladnoi Spektroskopii, Vol. 90, No. 5, pp. 738–746, September–October, 2023. Original article submitted June 7, 2023.



The purity of the dyes samples was checked by LC/MS using an Agilent 1200 Rapid Resolution LC with an Agilent 6410 Triple Quad mass spectrometer and a diode array detector. The solvents were ethanol, chloroform, and *o*dichlorobenzene (*o*-DCB) purified according to standard procedures [15]. Tetrabutylammonium bromide, a salt soluble in organic solvents, was additionally introduced during the experiments in order to increase the concentration of Br⁻ anions while maintaining constant dye concentration.

The fluorescence characteristics of the dyes were recorded using a Horiba Scientific Fluorolog spectrofluorimeter (USA, France, Japan), while the electronic absorption spectra were taken on either a Solar PV 1251B spectrophotometer (Belarus) or Proscan MC 122 spectrophotometer (Germany). The measurements were carried out with variation of the dye concentration in the range from 10^{-8} to 10^{-3} M using cells with sample thickness 500.13 mm. Since the luminescence characteristics of the PD are temperature-dependent, the samples were maintained at constant temperature.

The singlet oxygen luminescence in the vicinity of 1270 nm was recorded using an apparatus constructed at the Photonics Laboratory of the Institute of Physics of the National Academy of Sciences of Belarus [16]. The measurement technique was described in our previous work [17]. The quantum yield for singlet oxygen formation (γ_Δ) was determined by a comparative method. The standards were 5,10,15,20-tetrakis(4-N-methylpyridyl)porphyrin in ethanol ($\gamma_\Delta = 0.77 \pm 0.04$) [18] and tetraphenylporphyrin (TPP) with $\gamma_\Delta = 0.74 \pm 0.05$ in chloroform. The emission of a semiconductor laser with $\lambda = 667$ nm was used for excitation. We measured the duration of singlet oxygen luminescence upon photosensitization by both the standards and compounds studied. The singlet oxygen luminescence lifetime was 12 ± 1 μs for the standard compounds in ethanol and 248 ± 6 μs in chloroform.

Results and Discussion. The shape of the spectrum and position of the maximum of the major absorption band remain unchanged in the concentration range from 10^{-8} to 10^{-5} M. The absorption spectra obey the Bouguer–Lambert–Beer law. The molar extinction coefficient $\varepsilon > 10^5$ M $^{-1} \cdot$ cm $^{-1}$ (Fig. 1, Table 1). The single-band fluorescence spectra of the dyes in ethanol are independent of the excitation wavelength. The fluorescence excitation spectra are identical in shape with the corresponding absorption spectra upon recording within the fluorescence band. The fluorescence quantum yield is independent of the solution concentration. The fluorescence attenuation kinetics of the dyes studied is approximated by a mono-exponential equation. The lifetimes are given in Table 1. Such properties of the dyes, on the one hand, confirm the purity of the samples and, on the other, are in accord with the hypothesis that the dye molecules are dissociated in polar solvents [2, 19].

The value of γ_Δ remains unchanged upon variation of the concentration of dyes PD1 (0.031 ± 0.005) and PD2 (0.050 ± 0.008) in ethanol in the range from $5 \cdot 10^{-8}$ to 10^{-5} M. The introduction of additional TBAB salt 10^{-2} M to ethanolic solutions of these dyes does not lead to change in γ_Δ . In previous work [20], we found similar behavior for the dye HITC with an unsubstituted chain in ethanol; $\gamma_\Delta = 0.006 \pm 0.001$ independently of the concentration.

Upon going to the low-polarity solvent chloroform, we find a significant increase in γ_Δ in the case of PD2 with increasing solution concentration: $\gamma_\Delta = 0.022 \pm 0.004$ when $C_{\text{dye}} = 2.6 \cdot 10^{-7} \text{ M}$ to $\gamma_\Delta = 0.104 \pm 0.016$ when $C_{\text{dye}} = 5.8 \cdot 10^{-5} \text{ M}$, an increase by a factor of 4.2 (Fig. 2). In this case, the $^1\text{O}_2$ phosphorescence decay time in this dye concentration range is $248 \pm 6 \mu\text{s}$. The $^1\text{O}_2$ phosphorescence decay time was recorded for dye PD1 proved independent of concentration while the singlet oxygen formation quantum yield also remained constant within experimental error $\gamma_\Delta = 0.032 \pm 0.003$. The efficiency of singlet oxygen formation by dye PD1 remains unchanged upon the introduction of TBAB ($C_{\text{TBAB}} = 10^{-2} \text{ M}$), which shifts the ionic equilibrium toward an increase in the fraction of contact ion pairs for this dye [21].

Signs of multicomponent behavior are not seen for dye PD1 in low-polarity chloroform in either the absorption or fluorescence spectra. Nevertheless, the molar extinction coefficient decreases from $2.6 \cdot 10^5$ to $2.2 \cdot 10^5 \text{ M}^{-1} \cdot \text{cm}^{-1}$ with increasing solution concentration from 10^{-8} to 10^{-5} M (Fig. 3a). In this case, there is no change in either the position of the maximum or the absorption band halfwidth. The shape and position of the fluorescence spectrum also remain unchanged

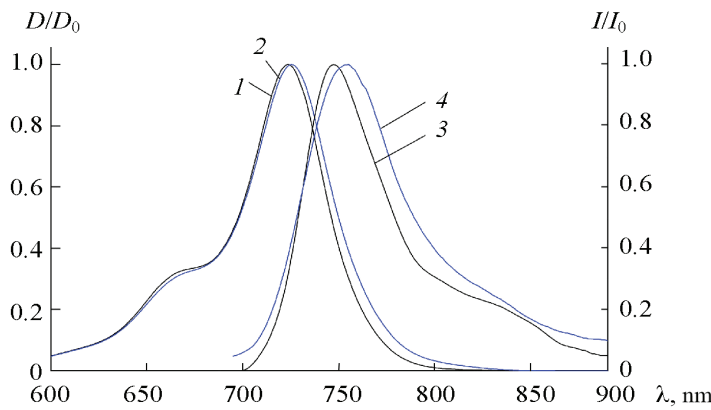


Fig. 1. Normalized absorption spectra (1, 2) and fluorescence spectra (3, 4) of dyes PD1 (1, 3) and PD2 (2, 4) in ethanol (dye concentration $5.0 \cdot 10^{-6}$ M).

TABLE 1. Photophysical Characteristics of Indotricarbocyanine Dyes

Solvent	Dye	C_{dye} , M	$\lambda_{\text{abs}}^{\max}$, nm	$\Delta\lambda_{\text{abs}}$, nm	$\epsilon \cdot 10^{-5}$, $M^{-1} \cdot cm^{-1}$	$\lambda_{\text{fl}}^{\max}$, nm	τ , ns	φ_{fl}	γ_{Δ}
Ethanol	HITC	$10^{-8} - 10^{-5}$	742	53	2.5	773	1.4	0.28	0.006
	PD2	$10^{-8} - 10^{-5}$	724	50	2.6	755	0.9	0.21	0.050
	PD1	$10^{-8} - 10^{-6}$	723	48	2.5	749	1.2	0.24	0.031
Chloroform	PD1	10^{-5}	732	50	2.1	763	1.6	0.23	0.032
	PD1	10^{-7}	732	50	2.4	761	1.6	0.23	0.032
	PD2	10^{-5}	780	93	1.4	763 807	1.5 2.1	—	0.104
	PD2	10^{-7}	736	95	1.5	763 807	1.5 2.1	—	0.022
Dichlorobenzene	PD1	10^{-5}	738	46	1.9	764	1.8	0.37	—
	PD1	10^{-7}	740	51	2.5	764	1.8	0.37	—
	PD2	10^{-5}	792	87	1.6	768 813	1.6 2.3	—	—
	PD2	10^{-7}	796	56	1.8	768	1.6	—	—

upon variation of the excitation wavelength (Fig. 4a); the quantum yield $\varphi_{\text{fl}} = 0.23$ and the fluorescence decay time was 1.6 ns. The kinetics of the fluorescence attenuation is approximated by a mono-exponential equation. The fluorescence polarization at $\lambda_{\text{exc}} = 650$ nm has a constant value of 8.5% upon recording within the fluorescence band. The shape of the fluorescence excitation spectrum is independent of the recording wavelength within the fluorescence band and is identical to the shape of the absorption spectrum. The addition of TBAB (10^{-2} M) to a solution of PD1 in low-polarity chloroform leads to a decrease in the molar absorption coefficient as in the case of increasing dye concentration (Figs. 3 and 4a). On the other hand, the quantum yield and fluorescence decay time as well as the efficiency of 1O_2 formation remain unchanged upon the introduction of TBAB.

Significant changes in spectral properties are observed for PD2 in going to low-polarity solvents — chloroform or DCB. Bands with maxima at 780 and 736 nm appear in the absorption spectrum of this dye in chloroform. Increasing dye concentration leads to an increase in the contribution of the short-wavelength band to the total absorption spectrum

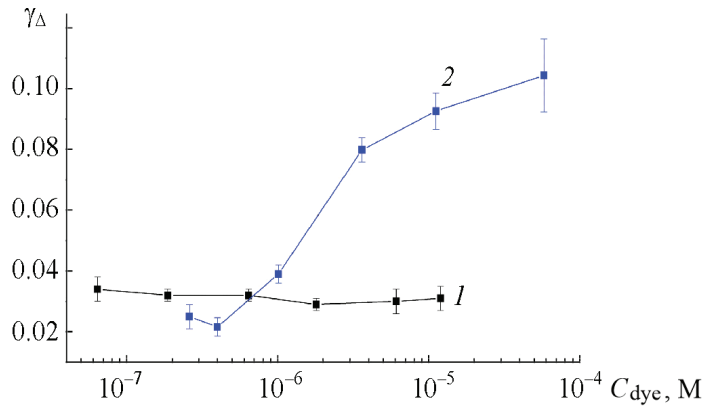


Fig. 2. Dependence of the singlet oxygen generation quantum yields of dyes PD1 (1) and PD2 (2) in chloroform on the dye concentration.

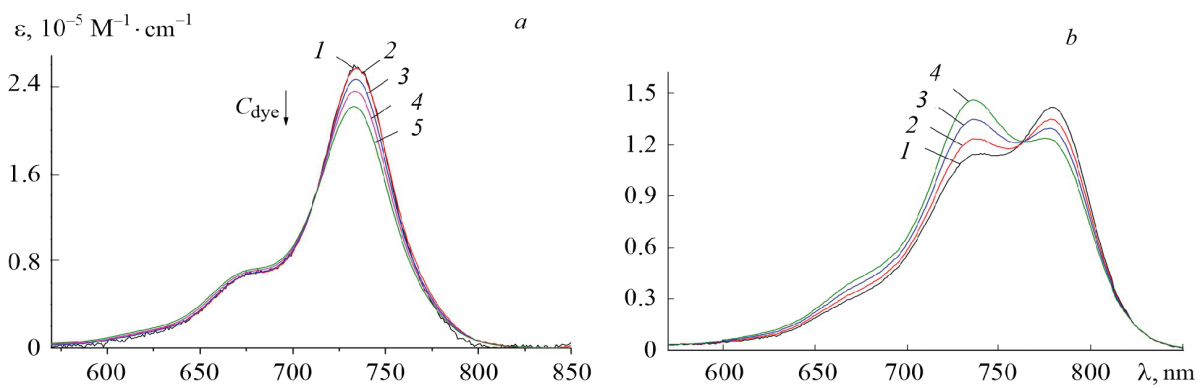


Fig. 3. Absorption spectra of PD1 (a) and PD2 (b) in chloroform at concentrations:
a) $6.4 \cdot 10^{-8}$ (1), $1.9 \cdot 10^{-7}$ (2), $6.4 \cdot 10^{-7}$ (3), $1.8 \cdot 10^{-6}$ (4), $6.1 \cdot 10^{-6}$ M (5); b) $5.0 \cdot 10^{-7}$ (1),
 $2.0 \cdot 10^{-6}$ (2), $8.0 \cdot 10^{-6}$ (3), $4.7 \cdot 10^{-5}$ M (4).

and a decrease in the long-wavelength region (Fig. 3b). The isosbestic point at $\lambda = 763$ nm indicates the existence of two absorption sites in the solution of PD2 in chloroform. The introduction of TBAB salt additive is accompanied by a decrease in the contribution of the band with maximum at $\lambda = 780$ nm in the absorption spectrum of dye PD2 (Fig. 4b).

The fluorescence spectrum of PD2 in chloroform has two bands, whose ratio depends on the wavelength of the excitation emission (Fig. 5b). Two maxima are found in the spectrum upon excitation in the range 600–720 nm: $\lambda_1 = 766$ nm and $\lambda_2 = 805$ nm. The fluorescence attenuation kinetic behavior differs when recording at these two maxima. Thus, the kinetics of fluorescence decay with $\lambda_{\text{rec}} = 740$ nm is approximated by a mono-exponential equation with decay time 1.5 nsec, while in the case of $\lambda_{\text{rec}} = 810$ nm, it is approximated by a bi-exponential exponential equation with decay times 1.5 and 2.1 ns. The fluorescence excitation spectrum with $\lambda_{\text{rec}} = 760$ nm shows bands in the short-wavelength region 300–500 nm, which are similar in shape and position to the bands in the absorption spectrum of the dye, as well as a band with maximum at 735 nm. Recording at the long-wavelength edge of the fluorescence spectrum gives still an additional strong band, whose position is identical to the position of the band at longest wavelength in the absorption spectrum. Similar changes in the photophysical properties of the dyes with variation in the concentration are seen for the other low-polarity solvent, namely, *o*-DCB (Table 1). On the whole, the absorption and fluorescence spectra for both dyes in DCB are shifted toward longer wavelengths in contrast to the spectra with chloroform as the solvent. In this case, evidence for the existence of two components is seen only for dye PD2.

Two segments with virtually invariant polarization are found in the polarization spectrum upon variation of the recording wavelength: 15.5–16.2% at 750–770 nm and 10.2–10.5% at 800–830 nm (Fig. 6). Since the measurements of the polarization were carried out at 18°C in liquid solutions and the values obtained under these conditions are a function of the ratio between the lifetime of the dye molecules in the excited state and the rotational relaxation time, i.e., the viscosity

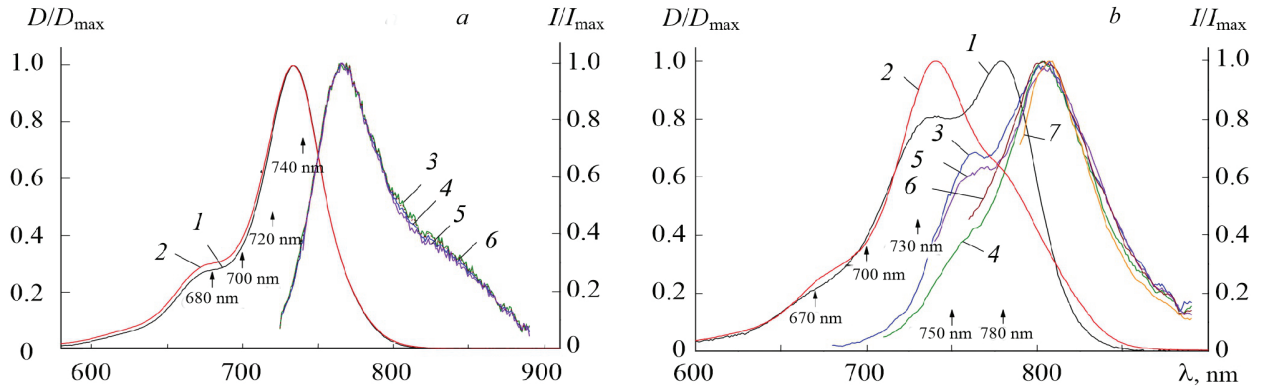


Fig. 4. Normalized absorption spectra [without salt (1) and with salt TBAB, $C = 10^{-2}$ M (2)] and fluorescence spectra of PD1 ($5.4 \cdot 10^{-7}$ M) in chloroform with excitation: a) $\lambda_{\text{exc}} = 680$ (3), 700 (4), 720 (5), 740 nm (6); b) $\lambda_{\text{exc}} = 670$ (3), 700 (4), 730 (5), 750 (6), 780 nm (7).

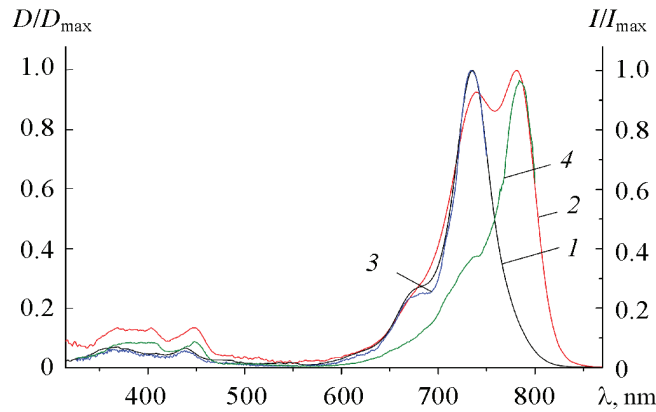


Fig. 5. Normalized absorption spectra of PD1 (1) and PD2 (2) in chloroform; fluorescence excitation spectra of PD2 in chloroform with $\lambda_{\text{rec}} = 760$ (3) and 810 (4).

of the solution, these data are in accord with the existence of two emitting components in the solution. In this case, the fluorescence decay time of the short-wavelength component $\tau = 1.6$ ns (mono-exponential kinetics for fluorescence decay at $\lambda_{\text{rec}} = 750$ nm), while the corresponding value for the long-wavelength component τ is 2.3 ns (biexponential kinetics for fluorescence quenching at $\lambda_{\text{rec}} = 810$ nm with decay times 1.6 and 2.3 ns). After the introduction of salt TBAB, the fluorescence spectrum displays only the short-wavelength component and the polarization proved to be independent of the recording wavelength (Fig. 6).

These spectral-luminescence data indicate the existence of two absorbing and fluorescing sites in solutions of dye PD2 in low-polarity solvents — chloroform and *o*-DCB, which can be assigned to different ionic forms of this dye [22–25], namely, contact ion pairs and free ions.

The differences in the spectral-luminescence properties of PD2 in low-polarity chloroform and *o*-DCB are related to shifts in the equilibrium state of the ionic forms of this dye in solution. Since the introduction of additional salt and increasing the dye concentration both lead to an increase in the fraction of contact ion pairs, the short-wavelength component in the absorption and fluorescence spectra of PD2 can be assigned to dye molecules present in solution as contact ion pairs, whereas the long-wavelength component can be attributed to free ions. The polarization spectra of PD2 in DCB recorded at $\lambda = 764$ and 812 nm offer irrefutable evidence for this interpretation (Fig. 7). A correlation is seen between the position of the extremes in the polarization and absorption spectra. The similar shape of the polarization spectra along with shifts in the position of the extremes suggests similarity of the position of the energy levels as well as identical symmetry of the emitting sites. This can be considered evidence for an equilibrium distribution of two types of ion pairs of PD2 in low-polarity

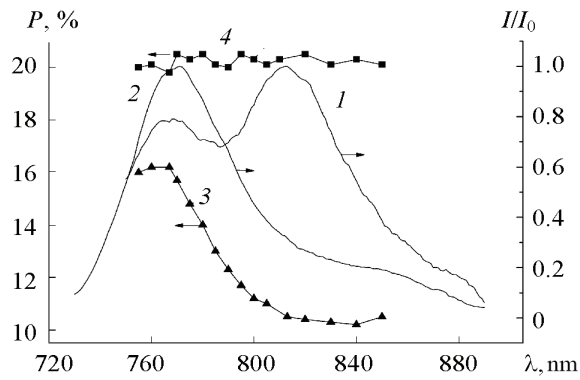


Fig. 6. Normalized fluorescence spectra (1, 2) and polarization spectra (3, 4) for PD2 in DCB (1, 3) and upon the introduction of salt TBAB (10^{-6} M) (2, 4), $\lambda_{\text{exc}} = 720$ nm.

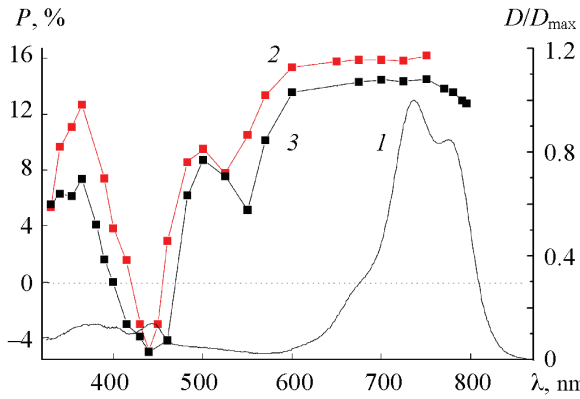


Fig. 7. Absorption spectrum (1) and polarization spectrum of PD2 in DCB at $\lambda_{\text{rec}} = 764$ (2) and 812 nm (3) at 14°C.

solvents. The decrease in the fluorescence anisotropy is especially pronounced upon excitation at the long-wavelength edge of the major absorption band when the selectivity of the excitation of the free ions is increased.

The increase in the singlet oxygen generation quantum yield for PD2 in low-polarity solvents with increasing dye concentration correlates with the increased fraction of its molecules as contact ion pairs. By analogy with the previously established behavior for the dye hexamethylindotricarbocyanine iodide (HITC) with anion Γ^- [20], the singlet oxygen generation quantum yield increases with increasing concentration due to greater conversion of molecules to the triplet state as a consequence of the heavy atom effect related to the bromide anion in this case [26–28].

The only weak dependence of the spectral-luminescence characteristics of dye PD1 in low-polarity chloroform on its concentration and upon the introduction of TBAB salt as well as the similarity with the spectral-luminescence characteristics of the contact ion pairs of dyes PD2 all suggest that dye PD1 in low-polarity chloroform exists predominantly as contact ion pairs. The molecular weight of the substituents consisting of two PEG chains is comparable to the molecular weight of dye PD1. Various workers [29–34] have studied the effect of the PEG configuration on the interaction of these molecules. Thus, Guo et al. [34] showed that the polyethylene glycol residues can envelop the individual molecules. It is precisely this property of PEG, which can be used to explain the existence of PD1 molecules in low-polarity solvents exclusively as contact ion pairs, suggesting the arrangement of the dye cation and anion in a single spatial cell. The significant difference in the singlet oxygen generation quantum yields of PD1 and PD2 under such conditions although both dyes exist predominantly as contact ion pairs (by a factor of not less than 2.5) is probably a consequence of the presence of the two PEG300 moieties on the terminal groups in PD1, which reduces the probability of collision of the chromophore of these molecules with dissolved oxygen, thereby hindering the sensitized formation of $^1\text{O}_2$.

Conclusions. This study of the spectral-luminescence and photophysical properties of indotricarbocyanine dyes has shown an increase in the singlet oxygen generation quantum yield γ_Δ for dye PD2 with increasing concentration in the range from 10^{-7} to 10^{-5} M: from $\gamma_\Delta = 0.022 \pm 0.004$ when $C_{\text{dye}} = 2.6 \cdot 10^{-7}$ M to $\gamma_\Delta = 0.104 \pm 0.016$ when $C_{\text{dye}} = 5.8 \cdot 10^{-5}$ M. On the other hand, we find a concentration-independent value $\gamma_\Delta = 0.032 \pm 0.003$ for PD1 with bulky substituents. The greater quantum yield of photosensitized singlet oxygen formation for PD2 in low-polarity chloroform is attributed to the greater fraction of contact ion pairs in solution with increasing concentration and the heavy atom effect of the anion. The two bulky polyethylene glycol chains with molecular mass 300 Da in the cationic indotricarbocyanine dye hinder escape of the counterion from the PD1 dye contact ion pair into the solution in the concentration range studied. The bulky substituents also hinder interaction of the dye chromophore with dissolved oxygen.

Acknowledgments. The authors express their gratitude to Candidates of Physical and Mathematical Sciences A. S. Stashevskii and V. A. Galievskii as well as Doctor of Physical and Mathematical Sciences Prof. B. M. Dzagarov at the Institute of Physics of the National Academy of Sciences of Belarus for consultation and assistance in carrying out the experiments with singlet oxygen.

This work was carried out with the financial support of the Belarusian Republican Foundation for Fundamental Research (Contracts F22UZB044 and F22MV914 both from May 4, 2022) and the State Scientific Research Programs (Project 3.03 Convergence2025 and Project 1.6 Photonics and Electronics for Innovations).

REFERENCES

1. E. S. Voropai and M. P. Samtsov, *J. Appl. Spectrosc.*, **65**, No. 2, 369–377 (1995); doi: <https://doi.org/10.1007/BF02606495>.
2. M. P. Samtsov, S. A. Tikhomirov, L. S. Lyashenko, D. S. Tarasau, O. V. Buganov, V. A. Galievsky, A. S. Stashevskii, and E. S. Voropay, *J. Appl. Spectrosc.*, **80**, No. 2, 170–175 (2013).
3. M. P. Samtsov, E. S. Voropai, K. N. Kaplevsky, D. G. Melnikau, L. S. Lyashenko, and Yu. P. Istomin, *J. Appl. Spectrosc.*, **76**, No. 4, 576–582 (2009).
4. A. A. Ishchenko and A. T. Syniugina, *Theor. Exp. Chem.*, **58**, 373–401 (2023); doi: 10.1007/s11237023097549.
5. D. M. Dereje, C. Pontremoli, M. J. Moran Plata, S. Visentin, and N. Barbero, *Photochem. Photobiol. Sci.*, **21**, 397–419 (2022); doi: 10.1007/s43630022001756.
6. N. Lange, W. Szlasa, J. Saczko, and A. Chwilkowska, *Pharmaceutics*, **13**, 818 (2021); doi: 10.3390/pharmaceutics13060818.
7. S. Kwiatkowski, B. Knap, D. Przystupski, J. Saczko, E. Kędzierska, K. Knap-Czop, J. Kotlińska, O. Michel, K. Kotowski, and J. Kulbacka, *Biomed. Pharm.*, **106**, 1098–1107 (2018); doi: 10.1016/j.biopha.2018.07.049.
8. E. S. Voropai, M. P. Samtsov, K. N. Kaplevskii, A. A. Lugovskii, and E. N. Aleksandrova, *J. Appl. Spectrosc.*, **71**, 180–186 (2004).
9. M. P. Samtsov, E. S. Voropai, D. G. Mel'nikov, L. S. Lyashenko, A. A. Lugovskii, and Yu. P. Istomin, *J. Appl. Spectrosc.*, **77**, No. 3, 406–412 (2010).
10. A. A. Lugovski, M. P. Samtsov, K. N. Kaplevsky, D. S. Tarasau, E. S. Voropay, P. T. Petrov, and Y. P. Istomin, *J. Photochem. Photobiol. A: Chem.*, **316**, 31–36 (2016); doi: 10.1016/j.jphotochem.2015.10.008.
11. M. P. Samtsov, D. S. Tarasov, A. S. Goryashchenko, N. I. Kazachkina, V. V. Zherdeva, A. P. Savitskii, and I. G. Meerovich, *Zh. Bel. Gos. Univ., Fizika*, No. 1, 33–40 (2018).
12. M. P. Samtsov, D. S. Tarasov, E. S. Voropai, L. S. Lyashenko, P. T. Petrov, V. M. Nasek, A. O. Savin, and R. D. Zil'berman, *Zh. Bel. Gos. Univ., Fizika*, No. 1, 19–26 (2019).
13. N. B. Bel'ko, M. P. Samtsov, and D. S. Tarasov, *Zh. Bel. Gos. Univ., Fizika*, No. 3, 17–23 (2020).
14. D. S. Tarasov, M. P. Samtsov, and N. N. Krasnoperov, *Zh. Bel. Gos. Univ., Fizika*, No. 2, 4–11 (2022).
15. A. J. Gordon and R. A. Ford, *The Chemist's Companion*, Wiley, New York (1972).
16. A. S. Stashevskii, V. A. Galievskii, and B. M. Dzagarov, *Pribory Metody Izmerenii*, **2**, No. 1, 25 (2011).
17. K. N. Kaplevskii, M. P. Samtsov, A. S. Stashevskii, V. A. Galievskii, D. S. Tarasov, and E. S. Voropai, *Vestn. Bel. Gos. Univ., Ser. 1: Fiz. Mat. Inform.*, No. 2, 7–11 (2012).
18. P. K. Frederiksen, S. P. McIlroy, C. B. Nielsen, I. Nikolajsen, E. Skovsen, M. Jørgensen, K. V. Mikkelsen, and P. R. Ogilby, *J. Am. Chem. Soc.*, **127**, 255–269 (2005); doi: 10.1021/ja0452020.
19. M. P. Samtsov, E. S. Voropai, K. N. Kaplevskii, and D. G. Mel'nikov, *J. Appl. Spectrosc.*, **75**, No. 5, 692–699 (2008).

20. M. P. Samtsov, D. S. Tarasau, A. S. Stashevskii, K. N. Kaplevsky, and E. S. Voropay, *J. Appl. Spectrosc.*, **81**, No. 1, 214–221 (2014).
21. E. S. Voropai, M. P. Samtsov, and K. N. Kaplevskii, *J. Appl. Spectrosc.*, **70**, 721–728 (2003).
22. T. Welton and C. Reichardt, *Solvents and Solvent Effects in Organic Chemistry*, John Wiley & Sons, Weinheim (2011).
23. I. R. Gould, R. H. Young, R. E. Moody, and S. J. Farid, *J. Phys. Chem.*, **95**, No. 5, 2068–2080 (1991).
24. X. Yang, Z. Zaitsev, B. Sauerwein, S. Murphy, and G. B. Schuster, *J. Am. Chem. Soc.*, **114**, No. 2, 793–794 (1992); doi: 10.1021/ja00028a075.
25. Y. Marcus and G. Hefter, *Chem. Rev.*, **106**, No. 11, 4585–4621 (2006); doi: 10.1021/cr040087x.
26. A. S. Tatikolov, L. A. Shvedova, N. A. Derevyanko, A. A. Ishchenko, and V. A. Kuzmin, *Chem. Phys. Lett.*, **190**, Nos. 3–4, 291–297 (1992); doi: 10.1016/00092614(92)853417.
27. A. V. Odinokov, M. V. Bazilevskii, N. Kh. Petrov, A. K. Chibisov, and M. V. Alfimov, *High Energy Chem.*, **44**, 376–382 (2010); doi: 10.2234/S0018143910050048.
28. V. A. Kuz'min, A. P. Darmanyan, V. I. Shirokova, M. A. Al'perovich, and I. N. Levkoev, *Izv. Akad. Nauk SSSR, Ser. Khim.*, No. 3, 581–586 (1978).
29. N. Derkaoui, S. Said, Y. Grohens, R. Olier, and M. Privat, *J. Colloid Interface Sci.*, **305**, 330–338 (2007); doi: 10.1016/j.jcis.2006.10.008.
30. B. Heymann and H. Grubmüller, *Chem. Phys. Lett.*, **307**, Nos. 5–6, 425–432 (1999), doi: 10.1016/S00092614(99)00531X.
31. Y. Hu, J. Xie, Y. W. Tong, and C. H. Wang, *J. Control. Rel.*, **118**, No. 1, 7–17 (2007); doi: 10.1016/j.jconrel.2006.11.028.
32. M. T. Peracchia, C. Vanthier, C. Passirani, P. Couvreur, and D. Labarre, *Life Sci.*, **61**, No. 7, 749–761 (1997), doi: 10.1016/S00243205(97)005390.
33. S. D. Li and J. Huang, *J. Control. Rel.*, **145**, No. 3, 178–181 (2010); doi: 10.1016%2Fj.jconrel.2010.03.016.
34. Y. Guo, H. Yuan, W. L. Rice, A. T. Kumar, C. J. Goergen, K. Jokivarsi, and L. Josephson, *J. Am. Chem. Soc.*, **134**, No. 47, 19338–19341 (2012); doi: 10.1021/ja309085b.